

## Theoretical Simulations of Chemical Behaviors in pH Modified Brines / Rock Interaction

K. Kato<sup>+</sup>, A. Ueda<sup>+</sup>, T. Sato<sup>++</sup>, M. Sato<sup>++</sup> and S.P. White<sup>+++</sup>

<sup>+</sup> Central Research Institute, Mitsubishi Materials Corp. 1-297, Kitabukuro-cho, Omiya, Saitama, 330-8508, Japan.  
koikato@mmc.co.jp, a-ueda@mmc.co.jp

<sup>++</sup> Geothermal Energy Research & Development Co., Ltd., Shinkawa Nittei Annex Bldg. 22-4, Shinkawa 1-Chome Chuo-ku, Tokyo 104-0033, Japan. msato@gerd.co.jp, okabe@gerd.co.jp, nakata@gerd.co.jp

<sup>+++</sup> Industrial Research Limited, Gracefield Road PO Box 31-310 Lower Hutt New Zealand. S.White@irl.cri.nz

**Keywords:** pH interaction, theoretical simulation, chemical behaviors, brine, rock

### ABSTRACT

Theoretical simulations have been performed to investigate chemical and mineral changes during the interaction of pH modified brine (pH 5.5) and reservoir rocks. Two types of models (porous and fracture) were examined using an improved ChemTough2 code for the kinetics of mineral precipitation/dissolution. In the vicinity of reinjection well, the brine pH increases to ~8 and the rock porosity decreases due to the precipitation of anhydrite. There is no appreciable difference in the chemistry of pH modified and non-modified brines.

### 1. INTRODUCTION

Silica scaling causes not only plugging trouble in surface pipeline like brine transportation lines, but also reduces the re-injection capacity. A number of methods for scale prevention have been proposed. It is well known that acid prevents silica scale by keeping brine pH low (Nishiyama et al., 1985). Scale deposition rates in the injection line were reduced and brine injectivity was also sustained by pH modification (Gallup, 1996). However, in the cases that brine contains high concentrations of silica or high salinity, pH modification is not always successful in preventing silica scaling.

This study aimed to simulate the effects of pH modification method in the reservoir and production well using the transport of reacting chemical simulator.

### 2. MODELLING SOFTWARE

For this work we have used a version of Tough2 (Pruess 1991) that has been modified to include the transport of reacting chemicals (White 1995). ChemTOUGH2 is a multi-component reactive flow code based on the porous media may be treated via the MINC formalism. ChemTOUGH2 will treat variably saturated multiphase reacting flows including those where boiling is taking place. Being based on TOUGH2 the discretization of the spatial domain is by the integrated finite difference method, which provides for modeling of 0-3 dimensional situations. Time stepping is fully implicit and heat and mass calculations are fully coupled with the reactive chemical calculations. Any number of chemical components (in solid, liquid or gas phases) and reactions may be included in the calculations. Reaction type available include: aqueous chemical complexation, redox reactions, gas dissolution-exsolution and mineral dissolution-precipitation. Mineral reactions

may be assumed to be either described by a general kinetic rate law or to be in local equilibrium. Activity coefficients of aqueous species are calculated using an extended Debye-Hückel formalism (Helgeson and Kirkham, 1974). Equations of state are available for CO<sub>2</sub> and CH<sub>4</sub>, all other gases are treated as perfect gases.

#### 2.1. Thermodynamic Data

The Soltherm database (Reed 1982) provides equilibrium constants as a function of temperature for all the reactions considered in this work up to a temperature of 350°C. It appears none of the widely available chemical databases provides data above this temperature explicitly. The program SUPCRT92 (Johnson *et. al* 1992) and associated databases provide a theoretical prediction of equilibrium constants for almost all the reactions of interest at temperatures up to 415°C. There is excellent agreement between theoretical predictions of SUPCRT92 and the Soltherm database in regions where they overlap.

#### 2.2. Water Rock Interaction

All reactions between the reservoir fluid and the minerals making up the reservoir are treated kinetically and we assume that the dissolution/precipitation reactions are surface reactions and so a rate equation consistent with transition state theory can be written as (Lasaga 1984)

$$R_j = A_j k \prod_i a_i^{n_i} f(\Omega) \exp\left(\frac{-E_a}{RT}\right) \quad (1)$$

where  $R_j$  is the reaction rate (Ms<sup>-1</sup>),  $A_j$  is the surface area available for mineral precipitation or dissolution (m<sup>2</sup>),  $k$  is the rate constant (Mm<sup>-2</sup>s<sup>-1</sup>),  $a_i$  the activity of species  $i$ ,  $f(\Omega)$  is some function of the saturation state of the solution,  $E_a$  is the activation energy of the reaction  $R$  the gas constant and  $T$  the temperature (°K). Catalytic or inhibiting effects of solution species are described by the  $\prod a_i$  term in Eq 1, in many cases all the  $n_i$  are zero and there are no catalytic or inhibiting effects by dissolved species. The functional dependence on the saturation state of the solution is given by

$$\Omega = \frac{Q}{K} \quad (2)$$
$$f(\Omega) = \text{sign}\left(1 - \frac{Q}{K}\right) \left(1 - \left(\frac{Q}{K}\right)^m\right)^n$$

where  $\text{sign}(x) = 1$  if  $x > 1$ ,  $= -1$  otherwise,  $Q$  is the ion activity product and  $K$  the thermodynamic equilibrium constant for the reaction,  $m$  and  $n$  are empirical constants to be determined experimentally, in this work they are both taken to be 1.0. Table 1 provides the initial parameters in this work.

The least constrained parameter in Eq 1 is the surface area available for reaction. The surface area exposed to fluid will depend on the nature of the permeability and may vary by several orders of magnitude between the extreme cases of flow in a few large fractures and flow in a large network of connected micro-fractures. Also, when a mineral not currently present in the rock assemblage becomes super-saturated some mechanism must be invoked to produce an initial surface area of the super-saturated mineral on which it may precipitate. Also when flow is predominantly in fractures, as is the case in many geothermal fields there may be 'armouring' of the fractures, effectively protecting much of the rock mass from exposure to injected fluid.

Steefel and van Cappellen (1990) discuss the role of nucleation and Ostwald ripening in the creation of surface area for the initiation of precipitation of super-saturated secondary minerals. They predict a very rapid increase in surface area once a nucleation threshold is exceeded with rapid reduction in super-saturation followed by a slower growth of the secondary mineral in the rock matrix. There are too many uncertainties in this work to make this level of detail appropriate so we adopt a simpler scheme. Once a secondary mineral becomes super-saturated by a specified amount we assume there is a spontaneous creation of surface area on which the mineral may precipitate and that precipitation rates are an order of magnitude greater than dissolution. Following Xu *et al.* (2001) the reactive surface area for the secondary minerals apart from the clays is set to 250 m<sup>2</sup>/m<sup>3</sup> of reservoir.

White (1998) discusses appropriate values for reactive surface area in fractured rocks and suggests that a value of 250 m<sup>2</sup>/m<sup>3</sup> or reservoir may be appropriate for a fractured reservoir. Xu *et al.* suggest a value of 1000 m<sup>2</sup>/m<sup>3</sup> is appropriate for sandstone and 100 m<sup>2</sup>/m<sup>3</sup> for fractured geothermal systems. Mroczek *et al* (2002) found even smaller values of about 5 m<sup>2</sup>/m<sup>3</sup> were required to match silica deposition about an injection well in an unspecified geothermal field. Given this wide range we perform two-dimensional simulations using surface areas of 100 m<sup>2</sup>/m<sup>3</sup>.

The surface area for each of the primary minerals is assumed to be proportional to the volume % of the mineral in the total mineral assemblage and this value changes as the calculation progresses.

### 3. MODEL DESCRIPTION

#### 3.1 Model Domain

We have chosen a very simple porous model, the aim being to investigate the parameters influencing the transport of low pH fluid from an injection area to a production area rather than produce a detailed model of a particular geothermal field.

Figure 1 show the Tough2 grid used in the simulation. The model represents a production / injection doublet with the injection and production areas spaced one kilometer apart. The reservoir is 100 meters thick. We set different type of parameters in production area and injection area. Table 2 provides the initial conditions of these areas. Before simulations begin, the reservoir pressure and temperature are 5 MPa and 250 C respectively.

#### 3.2. Chemical Species and Mineralogy

Modelling the transport of reactive chemicals is a computer intensive activity, and requires that a balance be struck between chemical complexity and calculation time. For this model, we have adopted a simplified subset of reservoir component species, including H<sub>2</sub>O, H<sup>+</sup>, Cl<sup>-</sup>, SO<sub>4</sub><sup>2-</sup>, HCO<sub>3</sub><sup>-</sup>, SiO<sub>2</sub>, Al<sup>3+</sup>, Ca<sup>2+</sup>, Fe<sup>2+</sup>, K<sup>+</sup> and Na<sup>+</sup>. These fluid components allow the modelling of reactions between the low pH injectate. 13 minerals included in the model are Albite-I, Anhydrite, Anorthite, Calcite, Enstatite, K-Feldspar, Kaolinite, Laumontite, Muscovite, Pyrophyllite, Quartz, Amorphous Silica, Wairakite.

Table 3 provides the setting parameters of chemistry and mineralogy in the model.

#### 3.3. Scenarios

We have investigated 2 cases with two-dimensional simulations in order to explore the effect of injectate pH on the time taken to neutralize injected fluid. Injectate chemistry was modified of injection water chemistry by adding sulfuric acid, which is calculated by geochemical simulator "WellChem" (White, 2000, Osawa 2002). Other parameters such as injection rate and the temperature are set to 600t/h, 120°C respectively. Table 4 shows the parameters in 2 cases.

### 5. RESULTS AND DISCUSSION

The simulation was running for 5 years. Figure 2 shows temperature contours after 2 years and 5 years. Temperature was decreased around an injection well. The effected area was about 150m from injection well. Figure 3 shows Cl<sup>-</sup> contours in each case after 2 and 5 years. A distribution of Cl<sup>-</sup> ion can use like a non-reacting tracer. There are two effects apparent in these figures, firstly the transport on injected species from the injection well to the production well and secondly boiling taking place about the production well concentrating chemical species already in the reservoir. The results show that the injection water is reached at least within 2 years.

Similar effects can be seen in the plots of pH with a plume of lower pH fluid moving towards the production area. In this case, however, H<sup>+</sup> is not transported as a non-reacting tracer but is neutralized by reaction with the reservoir minerals. Figure 4 shows the pH distribution in Case 1 and 2. Low pH area was distributed only near the injection well. Then the pH was rapidly increased to about 8.0. The pH distribution was caused by interactions with reservoir minerals and effect of temperature. After 5 years, injection water was reached to the production well. But the pH was almost neutralized, and we could not see a big difference between Case 1 and Case 2. We could not see the influence of pH modified injection water to the production well. Figure 5 shows Anhydrite distribution in each case. Anhydrite was precipitated around injection well. The effected area was restricted to near the injection well. Case 2 (pH 5.5 and 5years) shows the highest amount of Anhydrite precipitation. It is considered that the result is originated by an effect of pH adjustment using sulfuric acid. We also calculated porosity change (Figure 6). It shows that the porosity is decreased about 10% around the injection well.

These results show that the influence of pH modified injection water is restricted to near the injection well. In this simulation, we use porous media for reservoir model and set same permeability and porosity in each layer. Injection

water is diffused in all the directions and to have reacted with reservoir rock. Although injection water has reached to the production well, pH is already neutralized and a precipitation of scale does not find around the production well.

### 5.1. Fracture Model

In order to control the direction of fluid flowing, the permeability between the injection well and production well was increased to  $1.0 \times 10^{-9} \text{ m}^2$ . Simulated conditions are as follows. Injection rate : 200 t/h, pH : 5.5, Temperature 40 °C. Figure 7 shows  $\text{Cl}^-$  concentration by time series in several points between injection and production well. The  $\text{Cl}^-$  concentration in production well was increased after about 1 month. It means that the injection water has reached in about 1 month. The pH trend is shown in Figure 8. The pH was rapidly neutralized and was increased by a reaction with reservoir minerals. Anhydrite distribution is shown in Figure 9. Anhydrite was precipitated near the injection well. Anhydrite has precipitated in an order from the position near the injection well. The precipitation was dissolved again with progress of time. The reservoir temperature was getting low as pouring of injection water progresses. So the Anhydrite saturation is increased by moving the low temperature front. But the Anhydrite scaling can not find at the production well in one year.

## 6. CONCLUSION

Theoretical simulations had been performed to investigate chemical and mineral changes during interaction of pH modified brine (pH 5.5) and reservoir rocks. Two types models (porous and fracture) were examined using an improved ChemTough2 code for kinetic reactions in precipitation/dissolution of minerals. We have chosen a very simple porous model, the aim being to investigate the parameters influencing the transport of low pH fluid from an injection well to a production well. In porous media, the result shows that the influence of pH modified (Case 1) and original (Case 2) water is not so different and the effected area was restricted to near the injection well. The porosity was decreased about 10%, and the main cause of this decreasing is a precipitation of Anhydrite. We changed permeability between injection well and production well in order to express fracture model. Injection water could move to production area more rapidly. We could not also identify the pH and scaling problem near the production well in this model. These results show that the buffer capability of the reservoir in porous media is high enough in these conditions, and the effected area is restricted to near the injection well.

## REFERENCES

Gallup, D.: Brine pH modification scale control technology. GRC trans, **20** (1996)749-755.

Helgeson, H.C., and Kirkham, D.H.: Theoretical prediction of the thermodynamic behavior of aqueous electrolytes at high pressures and temperatures: II. Debye-Hückel parameters for activity coefficients and relative partial molal properties, American Journal of Science, **274**, (1974) 1199-1261.

Johnson, J.W., Oelkers, E.H., Helgeson, H.C.: SUPCRT92: A software package for calculating the standard molal thermodynamic properties of minerals, gases, aqueous species and reactions from 1 to 5000 bar and 0 to 1000 °C, Computers & Geosciences, **18** (1992) 7.

Lasaga, A. C.: Chemical kinetics of water-rock interactions, Journal of Geophysical Research, **89**, (1984) .4009-4025.

Mroczeck, E. K., White, S. P. and Graham, D. Estimating the quantity of silica deposited in the reservoir around an injection well, Proc. 24<sup>th</sup> New Zealand Geothermal Workshop (2002) 187-190.

Nishiyama, E., Hirowatari, K., and Kusunoki, K.: Study on injecting low temperature geothermal brine. GRC trans, **9**(2) (1985) 347-351.

Osawa, K., Sato, M., Okabe, T., Nakata, H. and White, S. P.: Development of a Wellbore Mineral Saturation Index Calculating Program WellChem, Proc. Geother. Res. Soc. Japan, (2002) B44 (in Japanese).

Pruess, K.: TOUGH2-A general purpose numerical simulator for multiphase fluid and heat flow Rep LBL-29400, Lawrence Berkeley Lab., Berkeley, Calif, (1991).

Reed, M. H.: Calculation of multi component chemical equilibria and reaction processes in systems involving minerals, gases and aqueous phase, Geochimica et Cosmochimica Acta, **46** (1982) 513-528.

Steefel, C. I. and van Cappellen, P.: A new kinetic approach to modelling water-rock interaction: the role of nucleation, precursors, and Ostwald ripening. Geochimica et Cosmochimica Act, **54** (1990) 2657-2677.

White, S.P.: Multiphase non-isothermal transport of systems of reacting chemicals. Water Resources Res. **31**(7) (1995) 1761-1772.

White, S.P., Lichiti, K. and Bacon, L.: Application of chemical and wellbore modeling to the corrosion and scaling properties of Ohaaki deep wells. Proceedings World Geothermal Congress, (2000) 3963-3968.

Xu T., Apps, J. A. and Pruess K.: Analysis of Mineral Trapping for  $\text{CO}_2$  Disposal in Deep Aquifers, Lawrence Berkeley National Laboratory Report LBNL-46992, (2001).

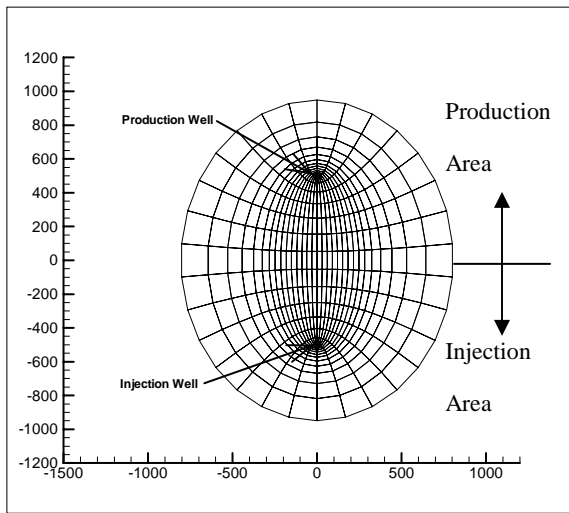


Figure 1: Tough2 grid used in flow modeling

Table 1 Initial kinetic property

Mineral	k25 (mol/m <sup>2</sup> /s)	Ea (J/mol)	m	n
anhydrite	3.10E-10	6.78E+04	1	1
calcite	3.10E-10	6.78E+04	1	1
albit-lo	3.10E-12	6.78E+04	1	1
anorthite	1.50E-12	6.78E+04	1	1
cristoblite-a	3.20E-13	6.91E+04	1	1
k-feldspar	3.10E-12	6.00E+04	1	1
kaolinite	1.00E-13	6.28E+04	1	1
laumontite	1.00E-12	7.28E+04	1	1
muscovite	2.36E-14	6.28E+04	1	1
pyrophyllite	1.00E-12	6.28E+04	1	1
quartz	1.26E-14	8.75E+04	1	1
amorphous silica	8.00E-13	6.28E+04	1	1
wairakite	1.00E-12	7.28E+04	1	1

Table 2 Setting parameters

Layer	Density (kg/m <sup>3</sup> )	Porosity (%)	Specific Heat (J/kg-deg.C)	Thermal Cond. (W/m- K)
Production Area	2,710	2	750	3
Injection	2,660	10	910	3.3
Layer				
		Permeability (mdarcy)		
		E-W	S-N	Vertical
Production Area	60	60	0.1	
Injection	10	10	1	

Table 3 Initial reservoir chemistry and mineralogy

Chemistry	
pH	5.6
Cl <sup>-</sup>	1.31e-2 mol/l
SO <sub>4</sub> <sup>=</sup>	1.02e-3 mol/l
HCO <sub>3</sub> <sup>-</sup>	2.06e-2 mol/l
SiO <sub>2</sub>	9.17e-3 mol/l
Ca <sup>++</sup>	4.11e-5 mol/l
K <sup>+</sup>	1.46e-3 mol/l
Na <sup>+</sup>	1.35e-2 mol/l
Al	1.85e-5 mol/l
Fe	8.95e-7 mol/l

Mineralogy		
Minerals	Production Zone	Injection Zone
Anhydrite	none	none
Calcite	2%	2%
Albit-low	25%	20%
Anorthite	25%	20%
Enstatite	5%	5%
k-Feldspar	13%	8%
Kaolinite	none	none
Laumontite	none	none
Muscovite	none	none
Pyrophyllite	none	none
Quartz	30%	45%
Amorphous Silica	none	none
Wairakite	none	none

Table 4 Injection conditions in 2 cases

Case	Injectate pH	Injection rate (t/h)	Temperature (deg.C)
1	5.5	600	120
2	7.5	600	120

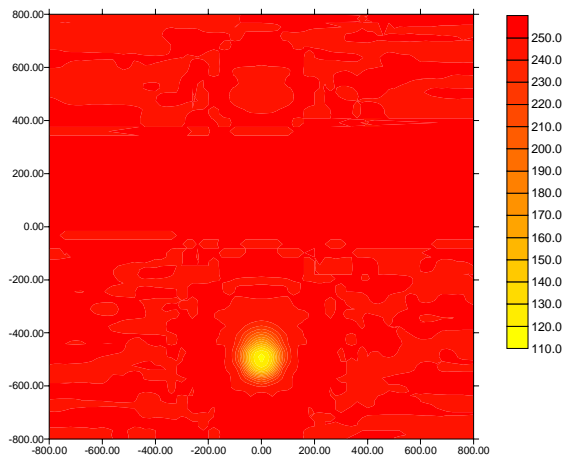


Figure 2a Temperature contour after 2 years

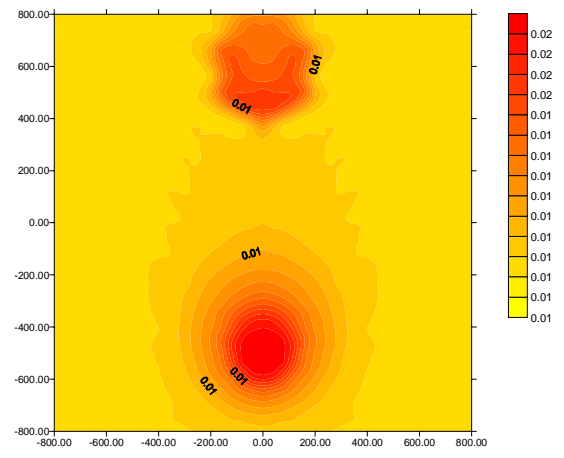
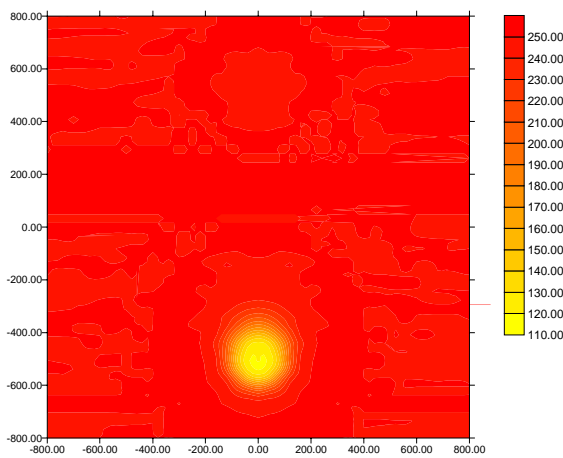
Figure 3b Cl<sup>-</sup> contour after 5 years

Figure 2b Temperature contour after 5 years

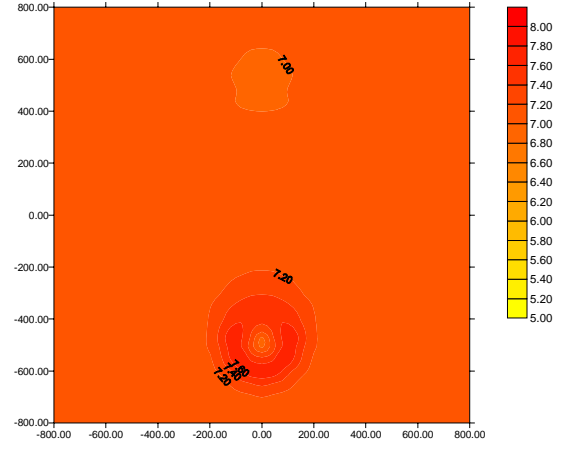


Figure 4a pH contour after 2 years in case 1

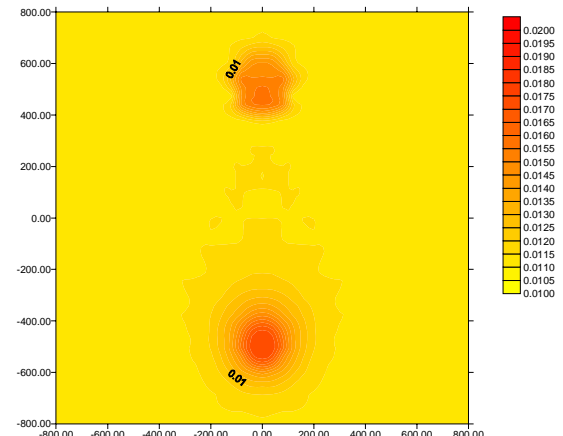
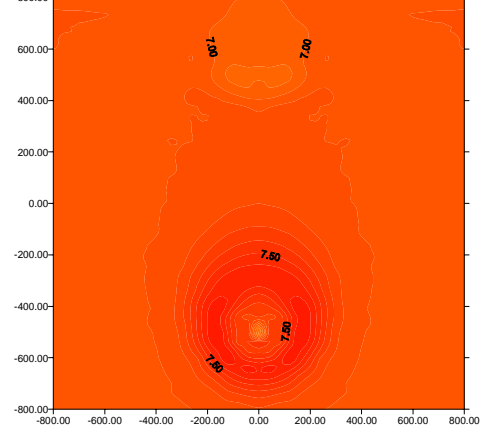
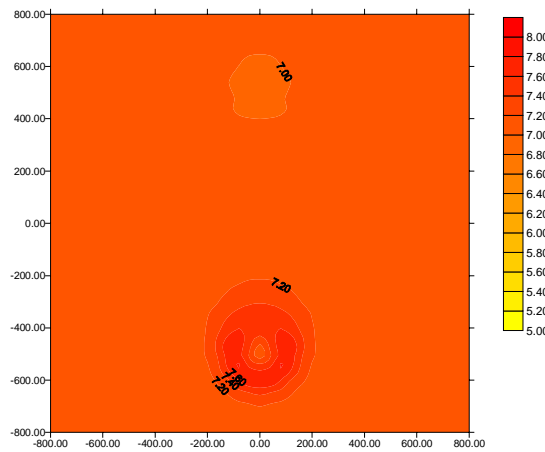
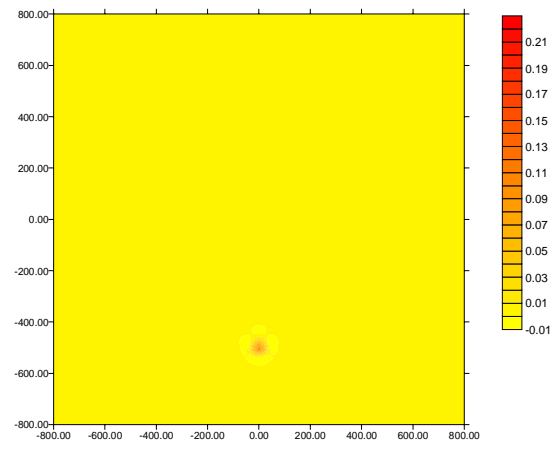
Figure 3a Cl<sup>-</sup> contour after 2 years

Figure 4b pH contour after 5 years in case 1



**Figure 4c** pH contour after 2 years in case 2



**Figure 5b** Anhydrite contour after 5 years in case 2

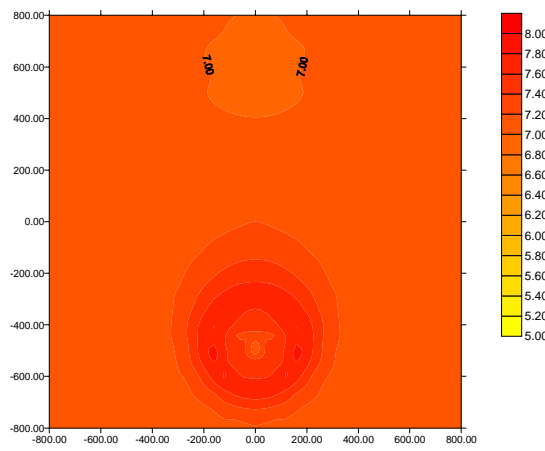


**Figure 4d** pH contour after 5 years in case 2

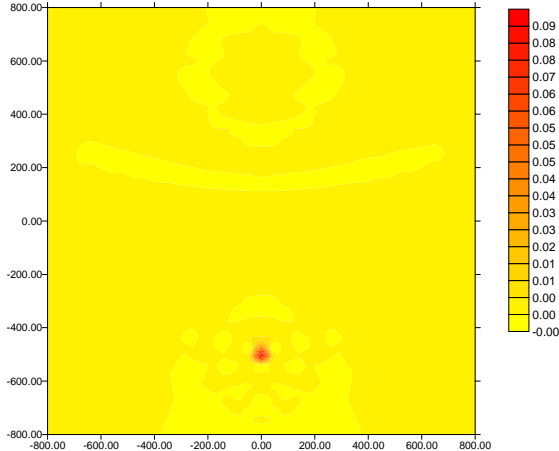


**Figure 6a** Porosity change after 5 years in case 1

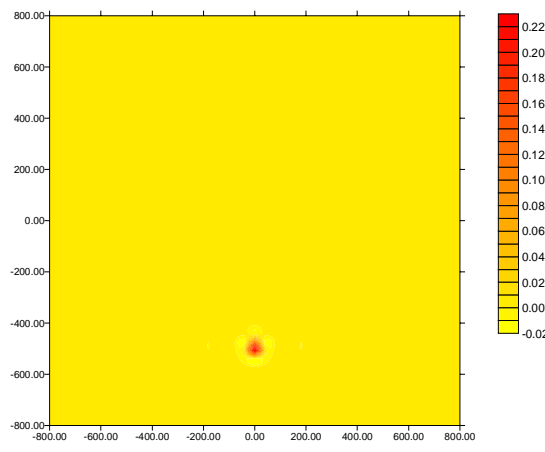


**Figure 5a** Anhydrite contour after 5 years in case 1

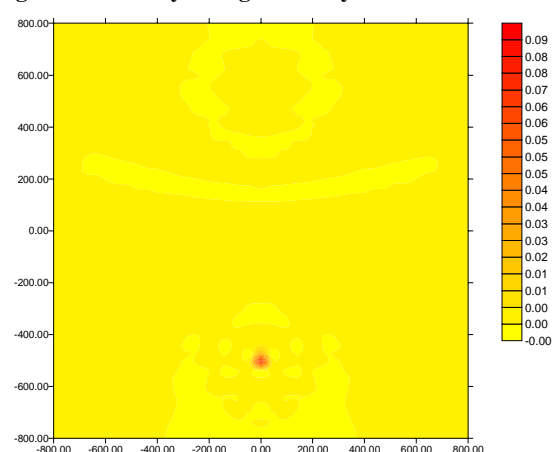


**Figure 6b** Porosity change after 5 years in case 2

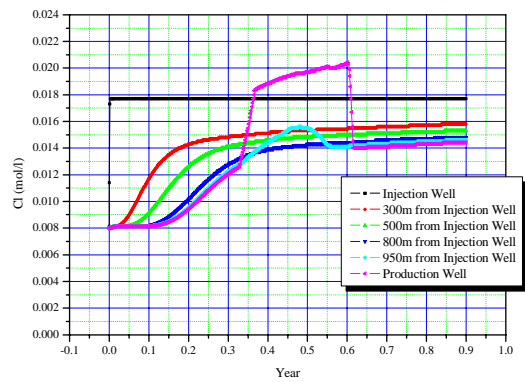
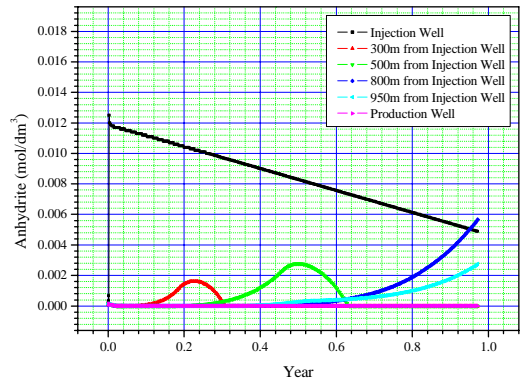
Figure 7 Time series of  $\text{Cl}^-$  concentration in 1 year

Figure 9 Time series of Anhydrite in 1 year

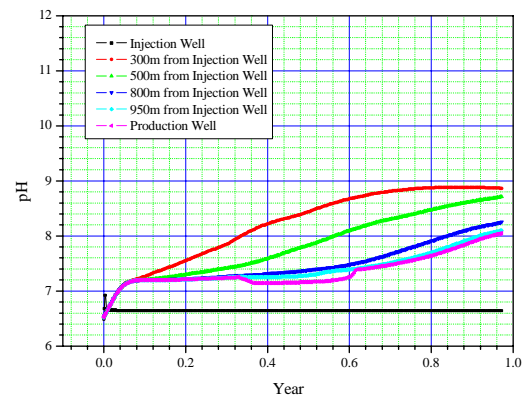


Figure 8 Time series of pH in 1 year